Taxus canadensis taxanes: structures and stereochemistry[1]

Lolita O. Zamir, Maria E. Nedea, Zhen-Hua Zhou, Sophie Bélair, Gaétan Caron, Françoise Sauriol, Emile Jacqmain, France I. Jean, François-X. Garneau, and Orval Mamer

Abstract: The structures and stereochemistry of 14 taxanes isolated from *Taxus canadensis* have been rigorously established by high-resolution NMR techniques and mass spectrometry. *Taxus canadensis* is the only yew that accumulates 9-dihydro-13-acetylbaccatin III (also called 7,9-deacetylbaccatin VI) as the most abundant taxane. Five 9-dihydrotaxanes derived from the Canadian yew are novel natural products not reported in the needles of other species of yew (**8–11**, **14**, Fig. 1).

Key words: *Taxus canadensis*, Taxaceae, taxanes, 9-dihydro-13-acetylbaccatin III, taxol.

Résumé : Les structures et la stéréochimie de 14 taxanes isolés du *Taxus canadensis* ont été rigoureusement prouvées à l'aide d'expériences à haute résolution de RMN et SM. *Taxus canadensis* est le seul if accumulant la 9-dihydro-13-acétylbaccatine III (aussi appelée 7,9-désacétylbaccatine VI) comme taxane majoritaire. Cinq 9-dihydrotaxanes dérivés de l'if du Canada sont des nouveaux produits naturels qui n'ont pas été découverts dans les aiguilles d'autres ifs (**8–11**, **14**, Fig. 1).

Mots clés : *Taxus canadensis*, Taxaceae, taxanes, 9-dihydro-13-acétylbaccatine III, taxol.

Introduction

Taxol (**1**, Fig. 1), the anticancer drug of the 1990s[3] was originally extracted from the bark of the Pacific yew, *Taxus brevifolia* (2). Two elegant total syntheses of taxol were recently reported (3, 4). Another very important drug, taxotere (which seems to be more active than taxol) (5), was derived by semi-synthesis: the natural product 10-deacetyl baccatin III (which is abundant in *Taxus baccata* (6, 7) and is very similar to the diterpenoid core of taxol) was chemically coupled at C-13 with a synthetic side chain. There are many reported syntheses of the side chain of taxol (8) and various derivatives are being made and tested.

In this publication we have focused on the Canadian yew, which differs from other yews not only in its physical appearance (it is a ramping small evergreen bush very common in Quebec), but also in its composition. *Taxus canadensis* does produce taxol, cephalomannine, and 10-deacetylbaccatin III (**1**, **4**, **5**, Fig. 1), which are common to all yews, as demonstrated by a major work of the National Cancer Institute research group (9). On the other hand, in a preliminary communication (1), we have shown that *T. canadensis* accumulates a taxane that differs from the diterpenoid core of taxol by a hydroxyl group at C-9, instead of a ketone: 9-dihydro-13-acetylbaccatin III (**7**, Fig. 1). This metabolite, which was reported in trace amounts in the bark of *Taxus chinensis* (10), is at least three to five times more abundant than taxol in the needles of *T. canadensis*. The structure that we proposed for this 9-dihydrotaxane, on the basis of NMR and MS data (**7**, Fig. 1), was subsequently confirmed by X-ray (11). This was an interesting finding, since the successful attachment of the taxol side chain by the Abbott group (12) led to in vivo anticancer activity. Further investigations in our laboratory with *T. canadensis* needles enabled us to rigorously characterize 14 taxanes. Five of these taxanes are new natural products that have not been reported in the needles of other yews (**8**, **9**, **10**, **11**, **14**, Fig. 1).

Received September 9, 1994.

L.O. Zamir,[2] M. E. Nedea, Z.-H. Zhou, S. Bélair, and G. Caron. Université du Québec, Institut Armand-Frappier, Centre de recherche en microbiologie appliquée, 531 boul. des Prairies, Laval, QC H7N 4Z3, Canada
F. Sauriol. Department of Chemistry, McGill University, 801 Sherbrooke Street West, Montreal, QC H3A 2K6, Canada.
E. Jacqmain. Jardin Botanique de Montreal, 4101 Sherbrooke Street Est, Montréal, QC H1X 2B2, Canada.
F.I. Jean and F.-X. Garneau. Université du Québec à Chicoutimi, 555 boul. de l'Université, Chicoutimi, QC G7H 2B1, Canada.
O. Mamer. Biomedical Mass Spectrometry Unit, McGill University, 1130 Pine Ave. West, Montreal, QC H3A 1A3, Canada.

[1] Presented in part as a communication (see ref. 1).
[2] Author to whom correspondence may be addressed. Telephone: (514) 687-5010, ext. 4260. Fax: (514) 686-5501.
[3] Taxol was recently approved in the U.S. and Canada for treatment of ovarian cancers.

Results and Discussion

Isolation and purification of taxanes

The discovery of a major taxane, 9-dihydro-13-acetylbaccatin III (**7**, Fig. 1), encouraged us to devise a method whereby this compound and taxol eluted in the same chromatographic fraction and could be easily separated. The choice of solvents and chromatographic techniques enabled us to obtain 9-dihydro-13-acetylbaccatin III at an R_t of 27.34 min, whereas taxol is obtained at R_t = 33.3 min on HPLC. Several steps of reverse-phase HPLC were usually needed to obtain highly pure tax-

Fig. 1. *Taxus canadensis* metabolites. Metabolites **2**, **3**, **6**, and **12** common to other *Taxus* species have been identified for the first time in *T. canadensis*. Metabolites **7**, **8**, **9**, **10**, **11**, **14** have not been found in the needles of other Taxus species.

(a) 9-Keto-Taxanes

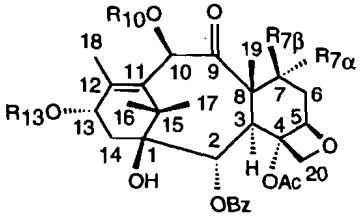

1 Taxol, R_{10}=Ac; $R_{7\beta}$=OH; $R_{7\alpha}$=H; R_{13}=PhCONHCH(Ph)CH(OH)CO

2 10-Deacetyltaxol, R_{10}=$R_{7\alpha}$=H; $R_{7\beta}$=OH; R_{13}=PhCONHCH(Ph)CH(OH)CO

3 7-Epitaxol, R_{10}=Ac; $R_{7\beta}$=H; $R_{7\alpha}$=OH R_{13}=PhCONHCH(Ph)CH(OH)CO

4 Cephalomannine, R_{10}=Ac; $R_{7\beta}$=OH; $R_{7\alpha}$=H; R_{13}=CH_3CH:$C(CH_3)CONHCH(Ph)CH(OH)CO$

5 10-Deacetylbaccatin III, R_{10}=$R_{7\alpha}$=R_{13}=H; $R_{7\beta}$=OH

6 7-Epi-10-Deacetylbaccatin III (10-Deacetyl-baccatin V), R_{10}=$R_{7\beta}$=R_{13}=H; $R_{7\alpha}$=OH

(b) 9-Dihydrotaxanes

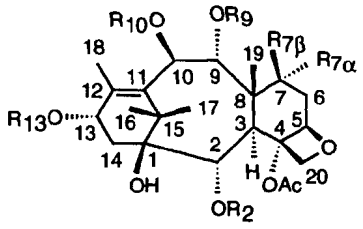

7 9-Dihydro-13-acetylbaccatin III R_2=Bz; $R_{7\beta}$=OH; R_9=$R_{7\alpha}$=H; R_{10}=R_{13}=Ac

8 7,9-Deacetylbaccatin IV R_2=R_{10}=R_{13}=Ac; $R_{7\beta}$=OH; R_9=$R_{7\alpha}$=H

9 10-Hydroxyacetylbaccatin VI R_2=Bz; R_9=R_{13}=Ac $R_{7\beta}$=OAc; $R_{7\alpha}$=H; R_{10}=$COCH_2OH$

10, 11 7-and 7Epi-9,10-Deacetylbaccatin VI R_2=Bz; R_7=β- and α-OH; R_9=R_{10}=H; R_{13}=Ac

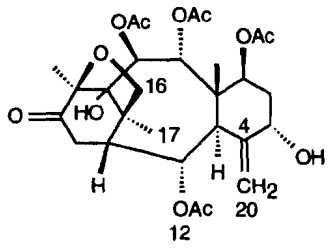

5-Decinnamate taxagifine

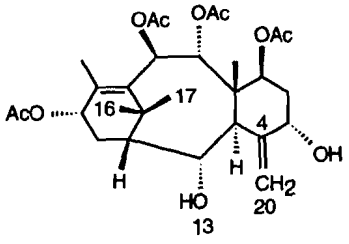

2-Deacetyl-5-Decinnamoyl taxinine J

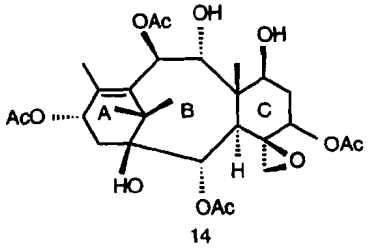

1β-Hydroxy-7, 9-Deacetyl baccatin I

anes. Purity of these taxanes was assessed by the formation of symmetrical peaks under three different gradient systems.

Taxanes isolated from *Taxus canadensis*

The structural characterizations of the taxanes were proven by high-field NMR techniques. High-resolution mass spectrometry confirmed the empirical formulas. Known taxanes were compared to the literature and spiked with standards for which we gratefully acknowledge the assistance of Ms Nancita Lomez and Dr. Kathleen H. Groover (National Cancer Institute, Maryland, U.S.A.). *Taxus canadensis* differs from other species of taxus by the presence of large amounts of the taxane

Table 1. Proton NMR, carbon NMR, and NOESY analyses of 7-epitaxol (metabolite **3**) isolated from *Taxus canadensis*. The ^{13}C assignments have been extracted from HMQC and HMBC. The stereochemistry was determined by NOESY.

Position	Parts/million	^1H NMR		NMR, δ	NOESY
		Multiplicity	*J*(Hz)		
				ppm	
1	---	---	---	78.93	
2	5.75	d	7.8	75.18	H-20, H-3, Me-17, Me-19
3	3.92	br d	7.3	40.19	H-10, H-2, Me-18, OH-7, Ac-4
4	---	---	---	81.83	
5	4.91	dd	9.3; 3.4	82.51	H-6, H-20, OH-7
6	2.29; 2.23	m	---	35.11	
7	3.693	br dd	10.2; 3.4	75.46	OH-7, H-6, Me-19, H-10
	4.68	d (OH-7)	11.7	---	H-5, H-3, H-7, Ac-4, Me-18
8	---	---	---	57.39	
9	---	---	---	207.38	
10	6.78	s	---	78.00	H-3, Me-18, OH-7
11	---	---	---	133.21	
12	---	---	---	139.43	
13	6.23	br t	8.8	72.07	Me-16
14	2.41	m		35.96	
	2.33			---	
15	---	---	---	42.47	
16	1.19	---	---	25.80	H-14B, H-13
17	1.14	---	---	21.00	Me-19, H-2, H-10
18	1.79	s	---	14.51	H-10, OH-7, H-3
19	1.66	s		15.92	H-7, H-20, H-2, Me-17
20	4.38	s	---	77.44	H-2, H-13, Me-19
NH	6.99	d	9.0		
H-3'	5.81	dd	9.3; 2.4	54.58	Ac-4, H-2', NH, Ph
H-2'	4.80	d	2.4	72.92	Ph, NH, H-3', Ac-4, Me-18
Ac-4	2.50	s		22.41	
Ac-10	2.19	s		20.72	
13(C=O)				172.57	
NH(C=O)				167.19	
Bz-2	8.17			130.20	
Bz-NH-3'	7.72			127.20	

9-dihydro-13-acetylbaccatin III (**7**, Fig. 1). We have therefore chosen to use the nature of the oxygenation at C-9 as the classification criteria.

A. 9-Keto-taxanes

We found taxol (**1**, Fig. 1), cephalomannine (**4**, Fig. 1), and 10-deacetylbaccatin III (**5**, Fig. 1) in *T. canadensis* needles.[4] We identified 10-deacetyltaxol (**2**, Fig. 1), 7-epitaxol (**3**, Fig. 1), and 7-epi-10-deacetylbaccatin III (**6**, Fig. 1) for the first time in the needles of the Canadian yew. These metabolites are known natural products isolated in other taxus species (13). The high-resolution 2D NMR analyses for 7-epitaxol and 7-epi-10-deacetylbaccatin III (**3** and **6**, Fig. 1) are shown in Tables 1 and 2.

B. 9-Dihydrotaxanes (7–14 Fig. 1)

Taxus canadensis is the only species accumulating 9-dihydro-13-acetylbaccatin III (**7**, Fig. 1) in its needles in quantities 3–5 times that of taxol. Structures **7** and **14** were identified subsequently as minor metabolites in the bark of *Taxus chinensis* (10) but were never found in yew needles. The taxane **12** was described in a Chinese publication (14) and compound **13** was also found in *Austrotaxus spicata* (15). The derivatives **8–11** have not been found in other taxus species. We can subdivide this group of 9-dihydrotaxanes into those with an oxetane ring (**7–11**, Fig. 1) and those with a pre-oxetane ring (double bond or C-4 epoxide such as **12–14** (Fig. 1). The initial characterization (1) of the abundant taxane (**7**, Fig. 1) involved 300 MHz NMR analysis and high-resolution mass spectrometry. The structure was confirmed by X-ray analysis (11). The 500 MHz NMR analyses of the new natural products are shown in Tables 3–7. The data for metabolite **7** are included for comparison. Compound **8** is very similar to the major metabolite **7**, the only difference being a substituent at C-2: an acetate replaces the benzoate. Compound **9** has a benzoyl at C-2 and a hydroxyl group on the acetyl at C-10 but otherwise is completely acetylated. Compounds **10** and **11** are stereoisomers differing in the stereochemistry at C-7. These compounds are the least acetylated, having three hydroxyl groups at C-7, C-9, C-10, a benzoyl at C-2, and an acetyl at C-13. The natural co-occurrence of these dihydrotaxanes (**7–11**, Fig. 1) suggests a biosynthetic order of acetylation, the first hydroxyl to be esterified being C-13 (and (or) C-4), followed by the one at C-2, then the other at C-10. The additional 9-dihydrotaxanes shown in Fig. 1 isolated for the first time in *T. canadensis* (1) have pre-oxetane structures on ring C. In compound **12**, ring

[4] We isolated a taxane that we characterized as 1-acetyl-10-deacetylbaccatin III (same structure as **5**, Fig. 1, but with OAc at C-1). The 500 MHz NMR and high-resolution mass spectral data were in agreement with the structure proposed. Unfortunately, we were only able to isolate this compound once!

Table 2. Proton NMR, carbon NMR, and NOESY analyses of 7-epi-10-deacetylbaccatin III (metabolite **6**) isolated from *Taxus canadensis*. The ^{13}C assignments have been extracted from HMQC and HMBC. The stereochemistry was determined by NOESY.

Position	Parts/million	^1H NMR		^{13}C NMR, δ	NOESY
		Multiplicity	*J*(Hz)	ppm	
1	---	---		---	
2	5.71	d	7.3	75.08	H-3, Me-17, Me-19, H-20B
3	4.05	d	7.3	40.37	H-2, H-10, H-6A/14A, Me-18
4	---	---	---	---	
5	4.94	dd	9.5; 3.7	82.37	H-6B
6A	2.37	m		38.33	
6B	2.23	o			
7	3.66	ddd	11.5; 4.6; 1.7	75.66	H-6A, Me-19
	4.87	d (OH-7)	11.5	---	H-3, H-7
8	---	---	---	---	
9	---	---	---	---	
10	5.49	s	---	78.29	H-3, Me-18
11	---	---	---	---	
12	---	---	---	---	
13	4.86	ot	7.7	67.79	Me-16, Me-18
14	2.34-2.25	m		35.12	
15	---	---	---	---	
16	1.07	---	---	19.37	H-13
17	1.08	---	---	26.37	H-2, Me-19
18	1.98	---	---	15.28	H-3, H-10, H-13
19	1.69			16.45	H-2, H-7, Me-17, H-20B
20A	4.41	d	8.8	77.71	H-2, Me-19, H-20B
20B	4.38	d	8.8		H-2, Me-19, H-20A
Ac	2.37	s		22.29	
Bz-2	---				
C1	---				
C2, 6	8.12	d	8.3	129.82	
C3, 5	7.50	t		128.46	
C4	7.62	t		133.42	

A is altered, with a cyclization containing a hydroxylated methyl (C-16 or C-17) on the double bond, assisted by an oxygenase.

High-resolution NMR analyses of *T. canadensis* taxanes

The detailed ^1H and ^{13}C assignments of all the metabolites reported for the first time in *T. canadensis* are shown in Tables 1–7. The 500 MHz NMR analyses utilized for all the new taxanes will be illustrated on the metabolite **14**, isolated for the first time in *T. canadensis*.

The proton NMR shifts and the COSY spectrum (16) allowed us to assign most of the protons. However, it was not possible to distinguish H-5 from H-7, H-10 from H-13, and H9/H10 coupled together could have reverse assignments. The four methyl groups could be identified by their couplings. The *gem*-dimethyl (Me-16 and Me-17) could be recognized by a small correlation in the COSY spectra. The methyl at position 19 (Me-19) showed a long-range coupling with H-3, and Me-18 with H-13/H-10. Three of the four acetyls of compound **14** could be easily located by the extra deshielding (~0.8–1 ppm) to the geminal proton (-C*H*-OAc) by comparison to an -OH (-C*H*-OH). These positions are H-2, H-10, and H-13. The position of the fourth acetyl was not immediately apparent.

The carbon-13 NMR assignments of the protonated carbons were established using the HMQC technique (*H*eteronuclear *M*ultiple *Q*uantum *C*oherence) (17) (Table 4). The carbon shifts that could not be determined were the quaternary carbons (C-1, C-4, C-8, C-11, C-12, C-15) and C-5, C-7, C-9, C-10, and C-13. Indeed, the signals of the attached protons (H-5/H-7; H-9/H-10; H-10/H-13) either overlap or are not assigned with certainty.

The additional heteronuclear correlation experiment HMBC (*H*etero *M*ultiple *B*ound *C*orrelation) (18) was therefore crucial for unambiguous assignment of all the carbons. The two-dimensional ^1H–^{13}C correlations for the four methyls are shown in Fig. 2*a*. The protons Me-16 and Me-17 are both correlated to C-15, C-11, and C-1. The protons Me-19 show coupling to C-8, C-9, C-7, and C-3 while methyl-18 correlates to C-13, C-11, and C-12. The HMBC experiment has also enabled us to corroborate the presence of the acetyls at C-10, C-13, and C-2. Indeed, in Fig. 2*b* we note that H-2, H-10, and H-13 are coupled to carbonyl groups. Surprisingly, we also note the most shielded proton (compared to H-13, H-10, H-2, H-9, H-7): a triplet at 4.2 ppm is correlated also to a carbonyl ester carbon (170 ppm). This triplet is also correlated to C-20, C-4, and C-3, confirming that it is indeed H-5. The higher chemical shift observed for H-5 on the acetylated C-5 position can be rationalized by the presence of an α-epoxide. The H-2 proton (Fig. 2*b*) also shows connectivities to six other carbons describing the total environment of that proton. These are C-1, C-14, C-15, C-3, C-4, and C-8 (the quaternary carbons that have not been assigned in HMQC are underlined). Among these quaternary carbons, C-15 and C-1 are assigned by analyzing the correlations of Me-16 and -17, which are coupled to

Table 3. Proton NMR analyses of 9-dihydrotaxanes (metabolites (*a*) **7–9**; (*b*) **10**, **11**, **14**.

(a)

Position	7	8	9
2	5.756 (d) J=5.9	5.471 (d) J=5.8	5.868 (d) J=5.9
3	3.05	2.91 (d)	3.159 (d)
5	4.954 (d) J=8.3	4.953 (d) J=8.7	4.959 (d) J=9.3
6A	2.55	2.53 (m)	2.487 (dt) J=8.3; 8.3; 15.1
6B	1.9	1.92 (o.m)	1.890 (o.m)
7	4.44 (o.m)	4.368 (o.m)	5.557 (dd) J=7.8; 9.3
9	4.44 (o.m)	4.383 (o.m)	6.027 (d) J=11.3
10	6.174 (d) J=10.7	6.122 (d) J=10.7	6.397 (d) J=11.3
13	6.163 (t) J=8.0	6.133 (o.m)	6.178 (br t) J=8.3
14A/14B	2.21(o.m)	2.25 (m)/2.00 (m)	2.22-2.19 (m)
16	1.249 (s)	1.233 (s)	1.223 (s)
17	1.676 (s)	1.605 (s)	1.744 (s)
18	1.946	1.911 (d) J=1.0 Hz	2.065 (d)
19	1.818	1.757 (s)	1.601 (s)
20A	4.309 (d) J=8.2	4.493 (d) J=7.8	4.332 (d) J=8.3
20B	4.161 (d) J=8.2	4.223 (d) J=7.8	4.117 (d) J=8.3
11'-A/11'-B	---	---	4.090 (J=16.6),4.027 (J=16.6)
Ac	---	2.159 (s)	2.294 (s)
Ac	2.276 (s)	2.156 (s)	2.202 (s)
Ac	2.190 (s)	2.124(s)	2.114 (s)
Ac	2.139 (s)	2.095 (s)	2.097 (s)
Benzoyl	H-ortho 8.1 ppm (d)	---	H-ortho 8.089 (d)
	H-meta 7.5 ppm (t)	---	H-meta 7.481 (t)
	H-para 7.6 ppm (t)	---	H-para 7.614 (t)

(b)

Position	10	11	14
2	5.828 (d) J=6.3	5.754 (d) J=5.9	5.331 (d) J=3.7
3	3.210 (d) J=5.8	3.058 (d) J=5.9	3.071 (d) J=3.7
5	4.926 (d) J=9.8	4.942 (od) J=7.8	4.202 (t) J=3.1
6A	2.6 (m)	2.54 (m)	2.038 (ddd) J=3.7, 12.0, 15.1
6B	1.8 (m)	1.9 (m)	1.887 (ddd) J=2.9, 4.4, 14.6
7	4.350 (dd) J=7.7, 10.3	4.364 (≈t)	4.253 (dd) J=4.6, 11.7
9	4.542 (d) J=10.3	4.306 (o.m)	4.591 (dd) J=4.4, 10.7
10	4.825 (d) J=10.3	4.924 (o.d) J=10.2	6.035 (d) J=10.7
13	6.182 (br t) J ≈5.8-7.3	6.190 (br t) J=7.3-9.3	6.051 (ddd) J=1.5, 6.6, 9.7
14A/14B	2.2 (o.m)	2.2 (o.m)	2.510 (dd) J=9.7, 14.9/1.864 (dd) J=6.6, 14.7
16	1.305 (s)	1.305 (s)	1.228 (s)
17	1.664 (s)	1.703 (s)	1.527 (s)
18	1.814 (s)	1.838 (d) J=1.0	2.157(d) J=1.5
19	1.58 (s)	1.810 (s)	1.388 (s)
20A	4.314 (d) J=8.3	4.306 (d) J=8.3	3.475 (d) J=5.4
20B	4.160 (d) J=8.3	4.166 (d) J=8.3	2.322 (d) J=5.4
11'-A/11'-B	---	---	---
Ac	2.288 (s)	2.278 (s)	2.184 (s)
Ac	2.183 (s)	2.185 (s)	2.134 (s)
Ac	---	---	2.099 (s)
Ac	---	---	2.051 (s)
OH-1	---	3.769 (s)	1.944 (s)
OH-7	---	3.283 (br s)	4.725 (s)
OH-9	---	4.870 (br d) J=7.2	3.574 (d) J=4.4
OH-10	---	3.193 (br s)	---
Benzoyl		8.078 (d) J=8.3	
		7.470 (t) J=7.7	
		7.600 (t)	

these two carbons, while the C-8 quaternary carbon is unambiguously identified from the Me-19 trace that is coupled to it (Fig. 2*a*). The H-9 proton, coupled to only one olefinic carbon (C-11), is also associated with C-10, C-7, C-8, and C-19, which describes the environment of this proton and confirms its assignment (Fig. 2*b*). The doublet of doublets located at 4.25 ppm is correlated to C-19 ($^3J_{C-H}$). This correlation allows us to definitely assign this proton as H-7. H-7 is also coupled to C-6 and C-5 (Fig. 2*b*). The connectivities in HMBC that enabled us to position the four acetates are shown in Fig. 2*c*.

The stereochemistry of the substituents, as well as the stereospecific assignment of Me-16 and Me-17, have been established using the NOESY experiment (NOE-2D) (19). In taxanes, despite their relative small size, the NOE cross peaks

Table 4. ^{13}C NMR analyses of 9-dihydrotaxanes (metabolites **7–14**).

Carbons	7	8	9	10	11	14
1	78.76	---	79.20	78.69	---	76.01
2	73.50	72.78	73.04	73.69	73.39	72.63
3	46.98	46.78	47.08	45.83	46.67	40.21
4	82.01	---	81.78	81.55	---	58.36
5	83.99	84.12	83.54	83.70	83.95	78.19
6	37.96	35.16	34.24	36.91	38.16	33.09
7	74.00	72.51 (or C-9)	71.58	72.26	74.27	69.60
8	45.00	---	46.10	41.54	---	46.52
9	76.85	73.89 (or C-7)	74.50	79.77	78.06	78.36
10	73.26	73.06 (or C-13)	71.87	~72	70.74	74.09
11	134.76	---	133.64	137.29	---	136.13
12	139.82	---	142.84	135.86	---	140.20
13	69.73	69.74 (or C-10)	69.54	69.76	69.86	71.16
14	35.33		34.83	35.11	35.23	38.61
15	43.00		42.79	42.97	---	43.39
16	28.28	27.96	28.12	28.32	28.18	28.43
17	22.57	22.15	21.99	21.89	22.02	22.05
18	14.88	14.68	14.70	14.00	14.68	15.48
19	12.48	12.19	12.37	12.00	12.33	13.54
20	76.56	76.66	76.25	76.55	76.61	49.88
Ac	22.84, 170.45	22.71	22.58, 169.69		22.60	21.70, 169.20
Ac	21.31, 170.23	21.05	20.83, 170.79		21.14	21.21, 169.80
Ac	21.29, 169.32	21.05	21.12, 170.43		---	21.38, 170.1
Ac	---	21.05	20.54, 170.79		---	20.92, 169.80
Benzoyl (CO)	167.04		167.48 (CO)		---	
C-1	128.67		128.75		---	
C-2, 6	130.08		130.21		129.96	
C-3, 5	128.64		128.75		128.61	
C-4	132.72		133.71		133.55	
10'	---	---	172.27			
11'	---	---	60.50			

Table 5. Comparison between ^{13}C chemical shifts for **10** and **11**. Most chemical shifts are similar (within 0.2 ppm) except for the ones shown in this table.

^{13}C	10	11	Difference (11-10)
C-3	45.83	46.67	Δ=0.8
C-6	36.91	38.16	Δ=1.2
C-7	72.26	74.27	Δ=2.0
C-9	79.77	78.06	Δ=1.7

are relatively strong. In these experiments, the NOE interactions are phased in an opposite fashion to the diagonal (negative phase), whereas the cross peaks originating from chemical exchange (OHs) are phased in a positive fashion. For the hydroxy protons we observe strong chemical exchange peaks (negative phase) and small NOE positive signals. In the NOESY tables (Tables 6, 7), only small positive NOEs (marked with an asterisk) are reported for these groups. Figure 3*a* illustrates the most informative NOEs, which rigorously establish the stereochemistry of ring A in compound **14**: we see that Me-16 points towards ring A and we can observe an NOE between Me-16, H-13 and 14A. Figures 3*b* and 3*c* show the most informative NOEs, which prove the stereochemistry of ring B from the β-side (Fig. 3*b*), and the α-side (Fig. 3*c*) of metabolite **14**. From Fig. 3*b*, we can conclude that Me-17, Me-19, H-2, and H-9 are on the β-side of the molecule **14**. On the other hand, in Fig. 3*c*, H-10, H-7, H-3, and Me-18 are on the α-side of compound **14**. The H-20A on the epoxide ring exhibits a small medium NOE with H-14B (α-orientation). The presence of this NOE suggests that the epoxide is β. For H-5, the vicinal coupling constants with its neighboring H-6 protons are small (J = 3 Hz), indicating a pseudo-equatorial orientation. The NOEs observed for H-5 are not very informative, since this proton interacts only with the vicinal H-6 protons and with H-20B. By molecular modelling we can identify two possible conformations for ring C shown in Figs. 3*d* and 3*e*. The twist-boat conformation of ring C (Fig. 3*d*) is characterized by a β-oxirane and an α-H-5. This configuration explains the observed coupling constants, as well as the NOEs (Fig. 3*d*). Indeed, the H-7 exhibits a large diaxial coupling with H-6A (ϕ = 174°) and a smaller coupling with H-6B (ϕ = 67°). The H-5 has two small couplings with H-6A (ϕ = 156°) and H-6B (ϕ = 37°). The H-5 and H-20B are close in space (≈2, 4 Å), explaining the strong NOE observed between these protons. Figure 3*e* represents a different possible conformation for ring C, which can also explain all the vicinal couplings and the NOEs observed. Indeed, in this chair conformation, the axial H-7 proton exhibits large diaxial coupling with H-6A and smaller axial-equatorial coupling with H-6B. The equatorial H-5 proton would show small couplings with the vicinal H-6A/H-6B. This configuration can also explain the observed NOEs and coupling constants. We can therefore conclude that the stereochemistry of H-5 could not be determined. On the other hand, the β-oxirane seems to be suggested by the data.

*Stereoisomers **10** and **11***

The stereoisomers **10** and **11** were first isolated in a 60:40 ratio. They were then separated and purified. The assignments are shown in Tables 3 and 4. The ^1H NMR of both compounds are very similar. The ^{13}C chemical shifts for both compounds appear at similar shifts (within 0.2 ppm), except for the car-

Fig. 2. Two-dimensional ^{1}H–^{13}C correlations obtained for metabolite **14**. Arrows indicate carbon–hydrogen connectivities. Arrow head indicates location of proton. Figure 2*a* shows the ^{1}H–^{13}C correlations for the four methyls. Figure 2*b* shows the ^{1}H–^{13}C connectivities that confirm the assignment of H-9. Figure 2*c* shows the ^{1}H–^{13}C correlations that led to the positioning of the four acetyls.

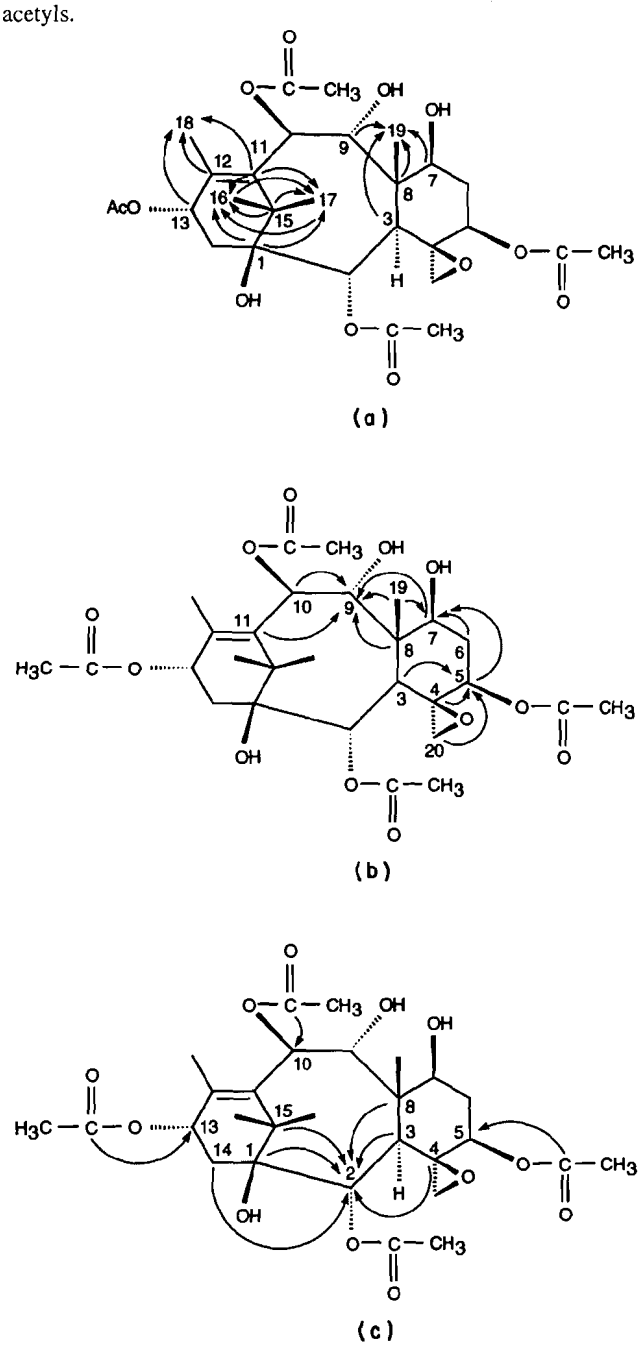

bons C-3, C-6, C-7, and C-9 (Table 5). The carbons showing these shifts are part of ring C (or close to ring C). In addition, the largest difference is at C-7, suggesting that they differ in the stereochemistry of C-7. Due to the similar NOEs we cannot conclusively determine in which stereoisomer the OH at C-7 is β and in which one it is α.

Mass spectra of *T. canadensis* taxanes

In the experimental section, the low-resolution and high-resolution mass spectra of taxanes are reported. The assignments of the different ions are also given. The results confirm our NMR data.

Experimental

High-performance liquid chromatography

Analytical high-performance liquid chromatography (HPLC) was carried out on a Perkin–Elmer instrument with an isocratic and binary LC pump model 250 coupled to a Waters 990 photodiode array detector, a NEC APC IV computer for data processing, and a Waters 990 plotter. HPLC was performed with two ODS-2 reversed phase columns (Whatman) connected in series (4.6 × 500 mm), at a flow rate of 1 mL/min. Sample injections were done manually using a 1.0 mL loop on a Waters UK6 injector. Separation was achieved with a linear gradient beginning with 75% water – 25% acetonitrile and increasing over 50 min to 100% acetonitrile. Semi-preparative HPLC was performed with two ODS-2 MAG-9 semi-preparative columns (Whatman) connected in series (9.4 × 500 mm), at a flow rate of 3 mL/min. The gradient program was the same, but it lasted either 70 min or 120 min. All ultraviolet detectors were set at 227 nm. All samples were filtered (0.45 μm) before injection. Water and acetonitrile were HPLC grade. The purity of all isolated products was checked by analytical HPLC. Semi-preparative HPLC was performed on a Waters Delta Prep 3000 instrument coupled to a Lambda-Max model 481 variable wavelength detector (Waters) and a Perkin–Elmer 024 recorder.

Nuclear magnetic resonance methodology

All the NMR spectra were obtained at room temperature on a UNITY-500 spectrometer operating at 499.843 MHz for proton and at 125.697 MHz for carbon-13. The NMR spectra were obtained on 1–2 mg samples dissolved in 0.3–0.4 mL of deuterated chloroform ($CDCl_3$). The solvent was used as an internal reference (77.0 ppm for ^{13}C and 7.25 ppm for ^{1}H). For the proton spectra, 8–64 transients were recorded with an 8000 Hz spectral window, 45° pulse, 30K data points, and 1.0 s acquisition time. The carbon-13 NMR spectra were obtained with a spectral window of 30 007.5 Hz, using a 40° pulse, and 50 000–70 000 transients were acquired. In cases were the concentration was too weak to obtain a good spectrum, the shifts were extracted from the HMQC experiment. The NOESY experiment (hypercomplex phase mode) was obtained using a mixing time of 0.3 s and a relaxation delay of 1 s. The acquisition was repeated for 16–32 transients, and 256 complex increments were acquired. The data were processed using a Gaussian apodization function. The final data matrix have 2K by 1K points (zero filling was used only in the evolution domain). For all the studies with taxol derivatives, when the diagonal signals are phased positive, the cross peaks resulting from dipolar relaxation (NOE) are phased negative, while the cross peaks originating from chemical exchange (OH) have positive phasing.

The HMQC experiment with a preceding BIRD nulling period was used with hypercomplex phased mode. The recycling delay was set to 1 s, while the nulling period (following the bird pulse) was set to 0.3 s. The acquisition was repeated 8–16 times and 256 fids were acquired. During acquisition of the proton spectra, C-13 broadband waltz decoupling was

Table 6. NOESY observed on the diastereoisomers **10** and **11**. In these experiments, the NOE cross peaks have a reverse phase (positive) relative to the diagonal (negative), whereas the chemical exchange cross peaks (hydroxy groups) are phased like the diagonal peaks. For the hydroxy protons we observed strong chemical exchange peaks (negative phase) and small NOE positive signal. In the table below, only the small positive NOEs are reported for these groups (*).

Proton	**10**	**11**
H-2	H-9 (w), Me-17 (s)	H-9 (s), Me-17 (s), Me-19 (m), H-20B (w)
H-3	H-7 (s), H-14 (m), Me-18 (w)	H-2 (w), H-7 (s), H-10 (w), H-14 (or Ac) (m), Me-18 (m)
H-5	H-6A (s), H-20A (s)	
H-6A	H-6B (s), H-5 (m), H-7 (m)	H-6B (s), H-5 (m), H-7 (m)
H-6B		
H-7	H-3 (m), H-6A (s), H-10 (m)	H-3 (s), H-6A (m), H-10 (s), Me-18 (m), OH-7 (w)
H-9	H-2 (w), Me-17 (s)	H-2 (m), Me-17 (s), Me-19 (m)
H-10	H-7 (m), Me-18 (m)	H-7 (m), Me-18 (m), OH-10 (w), H-3 (w)
H-13	H-14 (m), Me-16 (m), Me-18 (w)	H-14 (m), Me-16 (m), Me-18 (w)
H-14	H-13 (m)	
H-15		
H-16		H-13 (s), Me-17 (s), H-14 (w)
H-17		H-2 (s), H-9 (s), Me-16 (s)
H-18		H-3 (m), H-6A (m), H-7 (m), H-10 (s), H-13 (w), H-14 (w)
H-19		H-2 (s), H-9 (s), OH-9 (m), H20B (s)
H-20A	H-20B (s), Me-17 (m)	H-20B (s), H-5 (m)
H-20B	H-20A (s), Me-19 (m)	H-20A (s), Me-19 (s), H-2 (w)
Bz C-2/6		H-20A (m)
OH-7*		H-7 (m), H-6B (w)
OH-9*		H-9 (m), H-7 (w), Me-19 (m)
OH-10*		H-10 (m), H-14 (w)

Table 7. NOESY observed on metabolite **14** (NOE positive cross peaks).

Proton	NOE observed: s (strong), m (medium), w (weak)
H-2	H-9 (s), Me-17 (s), Me-19 (m), H-3 (w), OH-1 (w)
H-3	H-7 (s), H-14B (s), Me-18 (m), H-2 (w), H10/13 (w), H20A (w)
H-5	H-20B (s), H-6A (m-s), H-6B (m-s), H-9 (w)
H-6A	H-6B (s), H-5 (m), Me-19 (m)
H-6B	- - -
H-7	H-3 (m), H-10/13 (m), H-14B (m), Me-18 (m), H-6A (w), H-6B (w),OH-7 (w)
H-9	H-2 (s), Me-17 (s), OH-9 (w), Me-19 (w)
H-10/H-13	H-7 (s), H-14A (s), Me-16 (s), Me-18 (s), H-3 (w), H-9 (w)
H-13	- - -
H-14A	H-14B (v.s), H-13/10 (s), Me-16 (m)
H-14B/H-6B	H-6A (v.s), H-14A (v.s), H-3 (m), H-7 (m), H-20A (m), H-5 (m)
Me-16	H-10/H-13 (s), Me-17 (s), H-14A (m-w), Me18 (w)
Me-17 (1.51)	H-2 (s), H-9 (s), Me-16 (s)
Me-18 (2.151)	H-10/H-13 (s), H-7 (m), H-3 (m)
Me-19 (1.386)	H-2 (m), H-6A (m), H-9 (m), OH-7 (w)
H-20A	H-20B (v.s), 14B/6B (m-w), 6A (w)
H-20B	H-20A (v.s), H-5 (s)
OH-1*	H-2 (m), Me17 (m), Me16 (w)
OH-7*	H-7 (w), Me-19 (w)
OH-9*	H-9 (m), Me19 (w), H-10/13 (w)

applied. The data were processed with a Gaussian function with zero filling in the evolution domain (^{13}C). The final matrix size was 2K by 1K. The spectral window in the carbon domain was 120–140 ppm, while it was about 7–8 ppm in the proton domain. The HMBC experiment was acquired using similar conditions, but without the null period and without ^{13}C decoupling during acquisition. The τ delay to emphasize long-range coupling was set to 100 ms. Also, the carbon window was set larger to accommodate carbonyl carbons (180–200 ppm) in the carbon domain. The HMBC data were processed using a shifted Gaussian function and were displayed and plotted in an absolute value mode.

Mass spectrometry

Low-resolution xenon fast atom bombardment mass spectra were obtained in glycerol, except as noted, with a VG ZAB-HS instrument operated under the following conditions: resolution, 2000; atom energy, 8 kV at 1 mA beam current; scan range 1200–200 Da at 10 s/decade. The samples were dissolved in 0.2 μL of dimethyl sulfoxide in the stage before addition of 0.5 μL of glycerol. The 10 spectra obtained for each sample were averaged to reduce statistical variations.

High-resolution measurements were made similarly in glycerol–DMSO, at a resolving power of 12 000. The ions of interest were manually peak-matched against glycerol cluster

Fig. 3. (*a*) NOESY correlations about ring A of **14**; (*b*), (*c*) NOESY correlations establishing stereochemistry of ring B (β-face b, α-face c); (*d*), (*e*) Plausible conformations for ring C and NOESY correlations.

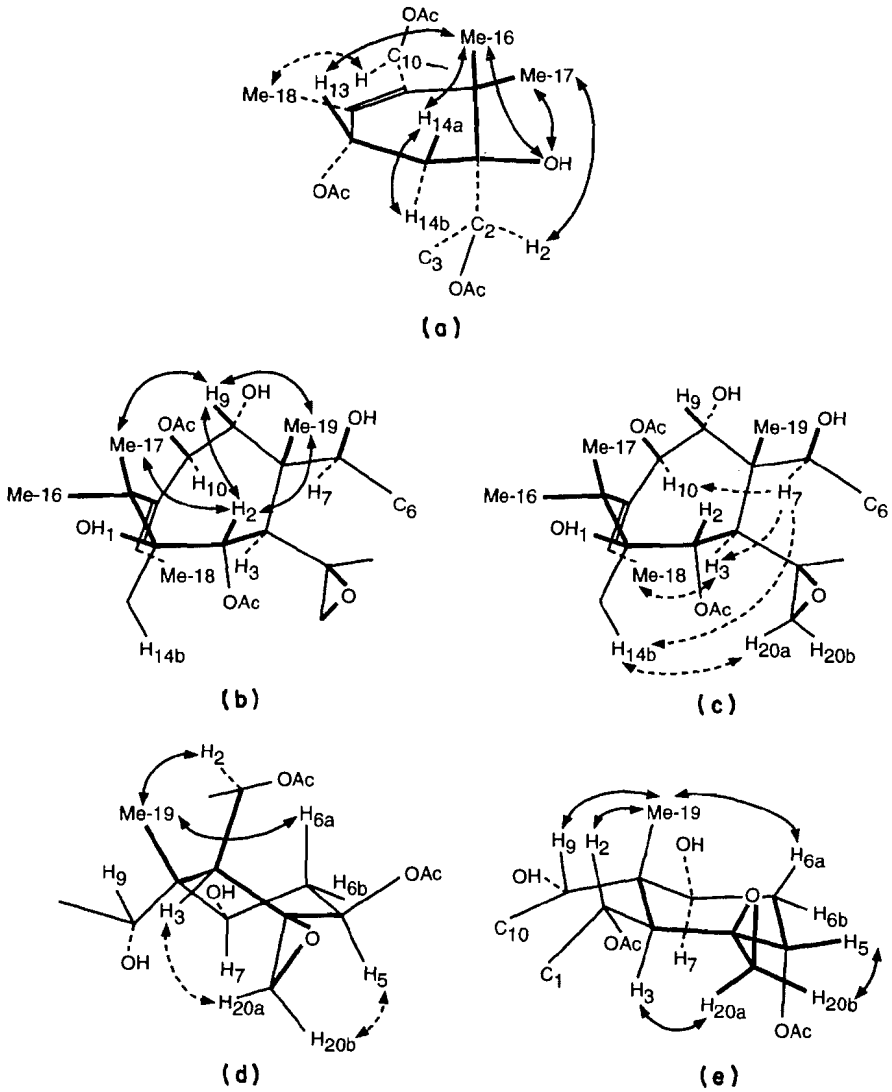

ions of known compositions, closest to the ions being measured.

IR spectroscopy

IR spectra were recorded using a Bruker IFS-48 FTIR spectrophotometer.

Circular dichroism

CD spectra were recorded using a Jasco J-500C spectropolarimeter with a 1.0 cm wide cuvette.

Plant material

Stems and needles of *Taxus canadensis* were collected at two different sites in Quebec. The material was stored at 4°C. When needed, they were dried at room temperature and ground in a blender for extraction.

Extraction, isolation, and purification of taxanes

Dried powdered needles and small branches of *T. canadensis* (480 g) were extracted twice with CH_3OH–CH_2Cl_2 (1:1, v/v, 4.8 L) during 24 h, at room temperature. The combined extracts were filtered and concentrated in vacuum to a dark brown residue. The residue was suspended in water and extracted with hexane to eliminate lipids. The aqueous layer was extracted with CH_2Cl_2 (3 × 300 mL) and the combined extracts were dried, filtered, and evaporated, giving a syrupy residue (18 g). The resulting extract was coated on Celite 545 and fractioned by flash chromatography on a silica gel column (150 g, 5 × 30 cm). The mixture was eluted with CH_2Cl_2–$CH_3COOC_2H_5$ (85:15) and then with a 5% step gradient starting with hexane–acetone (65:35) and ending with 100% acetone. Fractions eluted with hexane–acetone (65:35) contained taxol **1**, 7-epitaxol **3**, cephalomannine **4**, 9-dihydro-13-acetylbaccatin III **7**, 10-hydroxyacetylbaccatin VI **9**, 5-decinnamate taxagifine **12**, 2-deacetyl-5-decinnamoyl taxinine J **13**, and 1β-hydroxy-7,9-deacetylbaccatin I **14**. Further elution of the mixture with hexane–acetone (60:40) afforded mainly 10-deacetylbaccatin III **5**, and small amounts of 10-deacetyl taxol

2, 10-deacetylbaccatin V **6**, 7,9-deacetylbaccatin IV **8**, and 7,9,10-deacetylbaccatin VI **10** and **11**. For each peak, acetonitrile was removed by evaporation under vacuum and the remaining aqueous solution was lyophilized to yield white amorphous solids. The different taxanes were purified by repetitive HPLC runs, using gradient and isocratic conditions. The very pure taxanes were analyzed by high-resolution NMR and mass spectrometry.

*9-Keto-taxanes (**1–6**, Fig. 1)*

The 9-keto-taxanes were purified by repetitive HPLC runs. The preliminary purifications of compounds **1–6** involved semi-preparative HPLC with a gradient over 70 min of CH_3CN:H_2O (25:75) to 100% CH_3CN. The retention times under those conditions are the following: compound **1**, R_t = 36.2 min; **2** (same gradient but over 100 min), R_t = 44.5 min; **3**, R_t = 39.1 min; **4**, R_t = 34.5 min; **5** (same gradient but over 120 min), R_t = 24.2 min; **6** (same gradient but over 120 min), R_t = 34.5 min. These compounds were further purified by analytical HPLC with the same gradient, but over 50 min. The retention times and the overall yields of the pure taxanes are as follows: **1**, R_t = 33.29 min (0.016%); **2**, R_t = 29.15 min (0.0008%); **3**, R_t = 36.75 min (0.0013%); **4**, R_t = 32.43 min (0.002%); **5**, R_t = 19.68 min (0.015%); **6**, R_t = 25.15 min (0.0006%).

The NMR of **1–6** were identical to literature values (13). In addition, their structures were confirmed by high-resolution mass spectrometry: **1** (taxol) MH^+: 854.33850; $C_{47}H_{52}NO_{14}$ requires 854.33878; **2** (10-deacetyltaxol) MH^+: 812.32791; $C_{45}H_{50}NO_{13}$ requires 812.32821; **3** (7-epitaxol) MH^+: 854.33850; $C_{47}H_{52}NO_{14}$ requires 854.33878; **4** (cephalomannine) MH^+: 832.35435; $C_{45}H_{54}NO_{14}$ requires 832.35443; **5** (10-deacetylbaccatin III) MH^+: 545.23871: $C_{29}H_{37}O_{10}$ requires 545.23867; **6** (10-deacetylbaccatin V) $M + H^+ - 2H_2O$: 509.21758; $C_{29}H_{33}NO_8$ requires 509.21754; $MH^+ - H_2O - HOAc$: 449.19620; $C_{27}H_{29}NO_6$ requires 449.19641.

*9-Dihydrotaxanes (**7 – 14**)*

The purifications for all these taxanes involved (*i*) a semi-preparative HPLC with a gradient of acetonitrile (25–100%) in water over times specified for individual taxane followed when necessary by an isocratic run and (*ii*) analytical HPLC. The 500 MHz ^1H and ^{13}C NMR analyses and NOESY experiments for these 9-dihydrotaxanes are reported in Tables 3–7. The chemical structures of these metabolites were confirmed by mass spectrometry and low- and high-resolution data.

9-Dihydrotaxane **7**: IR (film) ν_{max}: 1743, 1714, 1371, 1245, 1179, 1111, 1053, 1018, 970 cm^{-1}; UV λ_{max} (CH_3OH): 228 nm (ϵ = 19 200); $[\alpha]_D^{22}$ −24.1 (c = 1.01, $CHCl_3$); [Θ] from CD (CH_3OH): +18.9 deg M^{-1} cm^{-1} at λ_{max} 252 nm and −8.6 deg M^{-1} cm^{-1} at λ_{min} 293 nm; MH^+: 631.27567; $C_{33}H_{43}O_{12}$ requires 631.27545. The retention time of **7** in semi-preparative HPLC with a gradient over 70 min, R_t: 39.10 min; analytical HPLC R_t: 27.34 min. The overall yield of **7** is 0.04%. Acetylation of metabolite **7** led to baccatin VI (9). The acetylation procedure is the following: 1 mg of **7** in dry pyridine (60 μL) was mixed with 90 μL acetic anhydride and stirred at room temperature overnight. Following removal of the pyridine, the acetylated product was purified by semi-preparative HPLC. Analyses of the NMRs of **7** and its acetylated derivative (1) established that metabolite **7** has hydroxyls at C-7 and C-9. In addition, the mass spectral data (low and high resolution) confirmed the structure of acetylated metabolite **7**: *m/z*: 715 (49.7%) MH^+: 715.29679; $C_{37}H_{47}O_{14}$ requires 715.29658); 697 (38.0%) ($MH^+ - H_2O$; 655 (90.8%) (MH^+ − AcOH); 637 (24.8%) (655−H_2O or 697−AcOH); 595 (60.7%) (655−AcOH); 535 (40.8%) (595 – AcOH).

9-Dihydrotaxane **8**: IR (film) ν_{max}: 1733, 1436, 1370, 1234, 1043, 1053, 1018, cm^{-1}; UV λ_{max} (CH_3OH): 217 nm (ϵ = 7400); $[\alpha]_D^{22}$ +24.05 (c = 1.83, $CHCl_3$); [Θ] from CD (CH_3OH): +32.9 deg M^{-1} cm^{-1} at ν_{max} 245 nm; *m/z*: 569 (35.9%) MH^+: 569.25989; $C_{28}H_{41}O_{12}$ requires 569.25980); 551 (29.6%) ($MH^+ - H_2O$); 509 (100%) (MH^+−AcOH), 491 (38.1%) (509−H_2O); 449 (37.3%) (509−AcOH); 431 (15.1%) (491−AcOH or 449 – H_2O). The retention time of **8** in semi-preparative HPLC with a gradient over 120 min, R_t = 20.5 min; isocratic CH_3CN:H_2O (26:74), R_t = 27.9 min; analytical HPLC R_t: 18.9 min. The overall yield of **8** was 0.0006%.

9-Dihydrotaxane **9**: IR (film) ν_{max}: 1734, 1374, 1245, 1099, 1052, 1027, 983, 803, cm^{-1}; UV λ_{max} (CH_3OH): 229 nm (ϵ = 13 653); [Θ] from CD (CH_3OH): 94.2 deg M^{-1} cm^{-1} at λ_{max} 290 nm; *m/z*: 753 (15.1%) (M + Na^+: 753.27357; $C_{37}H_{46}O_{15}Na$ requires 753.27344); 731 (5.7%) (MH^+); 713 (3.1%) ($MH^+ - H_2O$). The retention time of **9** in semi-preparative HPLC with a gradient over 70 min, R_t = 37 min; analytical HPLC isocratic CH_3CN:H_2O (42:58), R_t = 47.9 min. The overall yield of **9** is 0.0006%.

*9-Dihydrotaxanes **10** and **11***: UV λ_{max} (CH_3OH): 228 nm (ϵ = 12 600). The high-resolution NMR data of the two stereoisomers corresponding to **10** and **11** are shown in Tables 3–6. The stereochemistry of C-7 in both stereoisomers **10** and **11** could not be rigorously proven by NOESY experiments. The low- and high-resolution mass spectral data were identical for both. The Exact Mass for each compound was 589.26471: $C_{31}H_{41}O_{11}$ requires 589.26488. Both metabolites form a sodium adduct found *m/z* 611 and peaks corresponding to $MH^+ - H_2O$ at *m/z* 571. The retention time of **10** in semi-preparative HPLC with a gradient over 120 min, R_t = 30.3 min; isocratic CH_3CN:H_2O (28:72), R_t = 54.5 min. The retention time of **11** in semi-preparative HPLC with a gradient over 70 min, R_t = 25.5 min. In analytical HPLC isocratic compounds **10** and **11**, R_t = 23.85 min. The overall yield of **10** is 0.002% and of **11** is 0.0008%.

The detailed NMR analyses of **12** and **13** are shown in Tables 3 and 4. Since **12** and **13** are not new natural products, their structures were confirmed by rigorous NMR analyses, comparison with the literature, and low-resolution mass spectrometry. Metabolite **12** showed a weak (M+ H^+) peak at *m/z* 567 (7.2%), a prominent M+ H^+ − H_2O peak at *m/z* 549 (92.6%), and a sodium adduct at *m/z* 589 (M + Na^+); other peaks were at *m/z* 489 (549 – AcOH) (67.0%); 531 (549−H_2O) (6.1%); 429 (489 – AcOH) (29.5%); 507 (M+ H^+−AcOH) (18.7%); 467 (507 – AcOH) (25.8%). Metabolite **13** showed a sodium adduct at *m/z* 559 (14%) and a prominent peak at *m/z* 477 (M+ H^+ – AcOH) (68.7%) and at *m/z* 459 (477 – H_2O) (33.7%). The retention time of both **12** and **13** in semi-preparative HPLC with a gradient over 70 min is R_t = 25.5

min. They were separated in analytical HPLC: R_t of **12**: 23.55, and of **13**: 25.48 min. The overall yield of **12** and of **13** is 0.004%.

9-Dihydrotaxane ***14***: IR (film) ν_{max} : 1734, 1436, 1371, 1239, 1022, 979, 962 cm^{-1}; UV λ_{max} (CH_3OH): 220 nm (ϵ = 7500); $[\alpha]_D^{22}$ +65.84 (c = 0.571, $CHCl_3$); [Θ] from CD (CH_3OH): +57.2 deg M^{-1} cm^{-1} at λ_{max} 286 nm; MH^+: 569.25989; $C_{28}H_{41}O_{12}$ requires 569.25980. The fragmentation pattern shows the following peaks: *m/z*: 569 ($M + H^+$) (11.1%); 591 ($M + Na^+$) (12.5%); 551 ($MH^+ - H_2O$) (12.1%); 509 (569 − AcOH) (21.1%); 491 (551 − AcOH) (26.5%); 449 (569 − 2AcOH) (12.6%); 431 (551 − 2AcOH) (11.9%); 389 (MH^+ − 3AcOH) (24.7%); 371 ($MH^+ - H_2O$ − 3AcOH) (10.5%). The retention time of **14** in semi-preparative HPLC with a gradient over 70 min, R_t: 22.5 min; analytical HPLC, R_t: 21.05. The overall yield of **14** is 0.004%.

Acknowledgments

We thank the Natural Sciences and Engineering Research Council of Canada and the Canadian Breast Cancer Research Initiative for support of this work via operating grants to Lolita O. Zamir. La Fondation Armand-Frappier is acknowledged for a fellowship to G.C.

References

1. L.O. Zamir, M.E. Nedea, S. Bélair, F. Sauriol, O. Mamer, E. Jacqmain, F.I. Jean, and F.X. Garneau. Tetrahedron Lett. **33**, 5173 (1992); **33**, 6548 (1992).
2. M.C. Wani, H.L. Taylor, M.E. Wall, P. Coggon, and A.T. McPhail. J. Am. Chem. Soc. **93**, 2325 (1971).
3. R.A. Holton, C. Somoza, H.-B. Kim, F. Liang, R.J. Biediger, P.D. Boatman, M. Shindo, C.C. Smith, S. Kim, H. Nadizadeh, Y. Suzuki, C. Tao, P. Vu, S. Tang, P. Zhang, K.K. Murthi, L.N. Gentile, and J.H. Liu. J. Am. Chem. Soc. **116**, 1597 (1994); R.A. Holton, H.-B. Kim, C. Somoza, F. Liang, R.J. Biediger, P.D. Boatman, M. Shindo, C.C. Smith, S. Kim, H. Nadizadeh, Y. Suzuki, C. Tao, P. Vu, S. Tang, P. Zhang, K.K. Murthi, L.N. Gentile, and J.H. Liu. J. Am. Chem. Soc. **116**, 1599 (1994).
4. K.C. Nicolaou, Z. Yang, J.J. Liu, H. Veno, P.G. Nantermet, R.K. Guy, C.F. Claiborne, J. Renaud, E.A. Couladouros, K. Paulvannan, and E.J. Sorensen. Nature (London), **367**, 630 (1994); K.C. Nicolaou, C.F. Claiborne, P.G. Nantermet, A. Couladouros, and E.J. Sorensen. J. Am. Chem. Soc. **116**, 1531 (1994).
5. M.C. Bissery, D. Guénard, G. Guéritte-Voegelein, and F. Lavelle. Cancer Res. **51**, 4845 (1991).
6. V. Senilh, S. Blechert, M. Colin, D. Guénard, F. Picot, P. Potier, and P. Varenne, J. Nat. Prod. **47**, 131 (1984).
7. J.N. Denis, A.E. Green, D. Guénard, F. Guéritte-Voegelein, L. Mangatal, and P. Potier. J. Am. Chem. Soc. **110**, 5917 (1988).
8. I. Ojima, I. Habus, M. Zhao, M. Zucco, Y.H. Park, C.M. Sun, and T. Brigaud. Tetrahedron, **48**, 6985 (1992); I. Ojima, I. Habus, and M. Zhao. J. Org. Chem. **56**, 1681 (1991); J.-N. Denis, A. Correa, and A.E. Greene. J. Org. Chem. **55**, 1957 (1990).
9. K.M. Witherup, S.A. Look, M.W. Stasko, T.J. Ghiorri, G.M. Muschik, and G.M. Cragg. J. Nat. Prod. **53**, 1249 (1990).
10. S. Zhang, W.M. Chen, and Y.H. Chen. Yaoxue Xuebao, **27**, 268 (1992).
11. G.P. Gunawardana, U. Premachandran, N.S. Burres, D.N. Whittern, R. Henry, S. Spanton, and J.B. McAlpine. J. Nat. Prod. **55**, 1686 (1992).
12. L.L. Klein. Tetrahedron Lett. **34**, 2047 (1993).
13. D.G.I. Kingston, A.A. Molinero, and J.M. Rimoldi. Prog. Chem. Org. Nat. Prod. **61**, 10 (1993).
14. Z.P. Zhang, Z.J. Jia, Z.O. Zhu, Y.X. Cui, J.L. Cheng, and Q.G. Wang. Planta Med. **56**, 293 (1990).
15. L. Ettouati, A. Ahond, O. Convert, D. Laurent, C. Poupat, and P. Potier. Bull. Soc. Chim. Fr. 749 (1988).
16. J. Jeener. Ampère international summer school, Basko Polje, Yugoslavia. 1971; W.P. Ave, E. Bartholdi, and R.R. Ernst. J. Chem. Phys. **64**, 2229 (1975).
17. L.J. Müeller. J. Am. Chem. Soc. **101**, 4481 (1979); A. Bax, R.H. Griffey, and B.L. Hawkins. J. Magn. Reson. **55**, 301 (1983); M.R. Bendall, D.T. Pegg, and D.M. Doddrell. J. Magn. Reson. **52**, 81 (1983).
18. A. Bax and M.F. Summers. J. Am. Chem. Soc. **108**, 2093 (1986).
19. S. Macura and R.R. Ernst. Mol. Phys. **41**, 95 (1980).